

STRENGTH AND CYCLIC CRACK-GROWTH RESISTANCE OF THERMALLY DEFORMED ALLOYS OF THE Al–Mg–Sc SYSTEM

O. P. Ostash,^{1,2} R. V. Chepil,¹ V. A. Titov,³ S. L. Polyvoda,⁴
M. M. Voron,⁴ and V. Ya. Podhurska¹

UDC 539.43:669.71

We study the microstructure, phase composition, strength and plasticity characteristics, and crack-growth resistance under cyclic loading of thermally deformed (by extrusion, pressing, and rolling) castings of Al–Mg–Sc alloys (of the 1570 and 1545 types) with different magnesium contents obtained as a result of magnetohydrodynamic stirring of melt. It is shown that the grain size of the alloy after rolling and the amount of grain-boundary precipitates of intermetallic compounds decrease as the magnesium content of the alloy becomes lower. The mechanical characteristics of both alloys ambiguously depend on the procedure and temperature of thermomechanical treatment. It is shown that the parameter of structural strength of the investigated alloys (complexly determined by the characteristics of strength and fatigue crack-growth resistance) is higher than for the available Al–Mg–Sc, Al–Mg, and Al–Cu–Mg alloys. At the same time, its lowest value was recorded for the alloy with fine grains.

Keywords: aluminum alloys, extrusion, pressing, rolling, structure, structural strength.

Introduction

Aluminum alloys of the Al–Mg–Sc system are extensively used in machine-building and, in particular, in the aerospace engineering due to their high strength, plasticity, corrosion resistance, and weldability. The required level of strength is attained as a result of structural (grain refining), solid-solution, and dispersion hardening accompanied by alloying with transition metals, among which scandium is proved to be most efficient [1, 2]. In this case, for the improvement of corrosion resistance, weldability, and workability in the high-strength state, it seems reasonable to decrease the magnesium content in these alloys from 6–7 down to 4–5 wt.% [1, 3–5].

The properties of the alloys also strongly depend on the technology of casting. At present, one of the most promising technologies of casting is based on the application of magnetohydrodynamic (MHD) casting machines [5, 6].

The optimal strength and plasticity characteristics are attained after the extrusion, pressing, and rolling of castings. The chemical composition and structural-phase state may affect the strength and crack-growth resistance of deformed Al–Mg–Sc alloys under cyclic loading and, in particular, their fatigue threshold, in different ways [7]. Therefore, the structural strength of materials and, especially, of materials intended for aerospace applications (in the case where the damage tolerance concept is applied to their operation) depends on the optimal combination of the characteristics of strength and crack-growth resistance. It can be efficiently

¹ Karpenko Physicomechanical Institute, National Academy of Sciences of Ukraine, Lviv, Ukraine.

² Corresponding author; e-mail: fmidep17@gmail.com.

³ “I. Sikorsky Kyiv Polytechnic Institute,” National Technical University of Ukraine, Kyiv, Ukraine.

⁴ Physico-Technological Institute of Metals and Alloys, National Academy of Sciences of Ukraine, Kyiv, Ukraine.

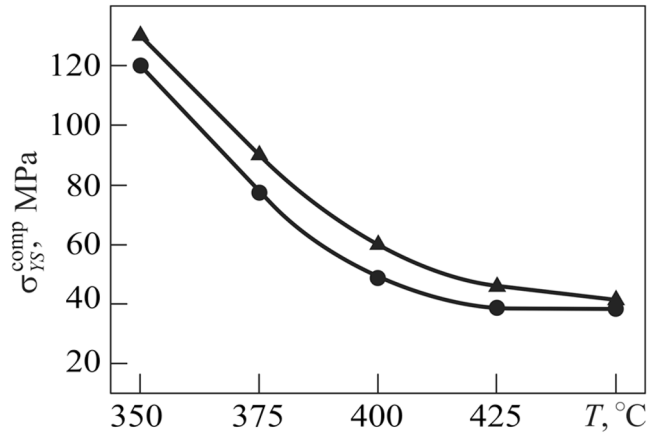


Fig. 1. Temperature dependences of the yield strength in compression for alloys No. 1 (●) and No. 2 (▲).

Table 1
Chemical Compositions (wt.%) of the Investigated Alloys

Alloy No.	Mg	Mn	Sc	Zr	Ti	Be	Fe	Si	Al
1	6.12	0.37	0.26	0.09	< 0.03	< 0.003	0.09	0.05	balance
2	4.85	0.32	0.24	0.12	< 0.03	< 0.003	0.08	0.04	

Comment: Here, we present averaged chemical compositions.

estimated [8, 9] by using the following complex parameter:

$$P = [\sigma_{UTS} \cdot \Delta K_{th} \cdot \Delta K_{fc}],$$

where σ_{UTS} is the ultimate strength; ΔK_{th} is the fatigue threshold, and ΔK_{fc} is the cyclic fracture toughness; these are the characteristics of fatigue macrocrack growth resistance (FMGR) of the material.

The aim of the present paper is to evaluate the structural strength of alloys of the Al–Mg–Sc system with various magnesium contents after thermomechanical treatment of castings obtained by using the MHD technology.

Material and Methods

We studied 1570- and 1545-type alloys [1] of the analyzed system with different magnesium contents (see Table 1). Castings with a diameter of 30 mm and a length of 150 mm were obtained as a result of MHD stirring of the melt at $700 \pm 10^\circ\text{C}$ with crystallization in a steel chill mold heated up to 300°C for the homogenization of their structure.

The resistance of the metal to plastic deformation was estimated according to the temperature dependence of the yield strength in compression $\sigma_{YS}^{\text{comp}}$ (Fig. 1) determined on standard specimens with a diameter of 10 mm

and a height of 23 mm cut out from the obtained castings. Therefore, the procedure of thermal deformation was performed by using different methods, namely, by the extrusion of castings with a diameter of 30 down to 20 mm at $390 \pm 10^\circ\text{C}$ (alloy No. 1) and $420 \pm 10^\circ\text{C}$ (alloy No. 2); by pressing of castings 30 mm in diameter into a strip 6 mm in thickness at $420 \pm 10^\circ\text{C}$, and by rolling of pressed blanks 20 mm in thickness into a plate with a thickness of 4.5 mm at $420 \pm 10^\circ\text{C}$ (alloy No. 1) or $460 \pm 10^\circ\text{C}$ (alloy No. 2).

For microstructural investigations, we used a Neophot-21 optical microscope and a Zeiss EVO-40XVP scanning electron microscope also used for the electron-probe microanalysis of the integral and local contents of alloying elements performed with the help of an INCA Energy-350 system for a diameter of the zone of electron-beam activation of about 4 μm .

The mechanical characteristics of the materials in tension (yield strength σ_{YS} , ultimate strength σ_{UTS} , and relative elongation δ_5) were measured on standard cylindrical specimens with a length-to-diameter ratio of 5:1 and a diameter of the working part equal to 5 mm and on plane specimens with the following cross-sectional sizes of the working part: 6×4.5 –6 mm.

The FMGR characteristics were established in tension for strip-like specimens ($150 \times 25 \times 4.5$ mm) and in three-point bending for beam specimens ($40 \times 8 \times 4.5$ mm) with sharp (with a radius of 0.1 mm) lateral notches 1–2 mm in length across the direction of rolling. The length of fatigue cracks was measured optically with an error of ± 0.01 mm. The tests were carried out at a frequency of 10–12 Hz for a load ratio $R = 0.1$ in air at 20°C . The dependences of the fatigue macrocrack growth rate da/dN on the SIF (stress intensity factor) range ΔK were plotted by using a standard procedure [10]. As the FMGR characteristics, we chose the fatigue threshold ΔK_{th} and cyclic fracture toughness ΔK_{fc} , i.e., the values of ΔK at $da/dN = 10^{-10}$ and 10^{-5} m/cycle, respectively.

Results and Discussion

As in the tests carried out at room temperature [5], the tests performed at $\leq 400^\circ\text{C}$ revealed a somewhat higher resistance of alloy No. 2 to plastic deformation as compared with alloy No. 1. Moreover, within the range 400 – 450°C , its changes were insignificant for both alloys (Fig. 1). A certain shift of this dependence for the as-cast alloy No. 2 toward higher temperatures as compared with alloy No. 1 can be explained by the composition of the secondary phase hardening the matrix: in alloy No. 2, this is an $\text{Al}_3(\text{Sc}_{1-x}\text{Zr}_x)$ intermetallic compound, whereas in alloy No. 1, this is Al_3Sc [5]. According to the literature data, alloys of the Al–Mg–Sc system are treated by thermal deformation within the range 300 – 480°C , although it is recommended to treat them at $\leq 420^\circ\text{C}$ [2]. Hence, in order to get a larger database, alloys No. 1 and No. 2 were investigated after extrusion, pressing, and rolling within the range 390 – 460°C (Table 2).

In the as-cast state, alloy No. 2 has better mechanical characteristics than alloy No. 1 (Table 2). After deformation treatment, these characteristics are substantially improved: σ_{YS} increases from 153–162 to 305–374 MPa; σ_{UTS} increases from 236–270 to 396–452 MPa, and δ increases from 11–15 up to 12–17% depending on the procedure of treatment. Thus, the highest strength was obtained for alloy No. 1 after multiple (eight runs) rolling and for alloy No. 2 after extrusion. The lower values of σ_{UTS} obtained for this alloy after rolling (Table 2) are probably caused by too high temperatures of treatment, i.e., the recommendation made in [2] that the optimal temperature should be $\leq 420^\circ\text{C}$ for alloys of this system is confirmed. The obtained results agree with the literature data (Table 2). Here, it should be noted that the thermally deformed alloys No. 1 and No. 2 reveal, as a rule, higher values of the yield strength σ_{YS} as compared to the value available from the literature, which may be caused by the positive influence of the MHD technology.

Table 2
Mechanical Characteristics of the Investigated Alloys in the As-Cast and Thermally Deformed States and Their Comparison with the Characteristics Known from the Literature

Alloy	Treatment	σ_{YS}	σ_{UTS}	$\delta_5, \%$
		MPa		
No. 1	Casting	153	236	11
	Extrusion (390°C)	310	397	12
	Pressing (420°C)	326	413	13
	Rolling (420°C)	374	450	12
No. 2	Casting	162	270	15
	Extrusion (420°C)	350	452	16
	Pressing (420°C)	309	405	16
	Rolling (460°C)	305	396	17
01570 [1] (5.8% Mg)	Extrusion	305–345	430–445	15–18
	Hot rolling	270–300	390–420	15–20
1570 C [3] (5.0–5.6% Mg)	Pressing and hot rolling	245–300	375–400	15–20
1575 C [12] (6% Mg)	Rolling (300°C, $\epsilon = 70\%$)	295	450	20
1545 [12] (4.57% Mg)	Rolling (360°C, $\epsilon = 70\%$)	280	385	20
1545 [13] (4.57% Mg)	Rolling (320–360°C)	260	395	17
	Cold rolling ($\epsilon = 20–70\%$)	375–450	440–490	8–10

Comments: For alloys No. 1 and No. 2, we present the averaged results of testing of at least three specimens.

The microstructures of alloys after rolling are noticeably different. The grain size across the direction of rolling is 50–150 μm in alloy No. 1 (Fig. 2a) and 50–100 μm in alloy No. 2 (Fig. 2b). In alloy No. 1, we recorded significant amounts of intermetallic compounds precipitating along grain boundaries, whereas, in alloy No. 2 with decreased magnesium content, their number is much lower. The data of local chemical analysis show (Figs. 2c, d) that, in both alloys, these were primary precipitations of intermetallic compounds: aluminum and magnesium; aluminum, manganese, and iron; aluminum, scandium, and zirconium (of the Al_3Mg_2 , $\text{Al}_6(\text{Fe}, \text{Mn})$, and $\text{Al}_3(\text{Sc}, \text{Zr})$ types) [11].

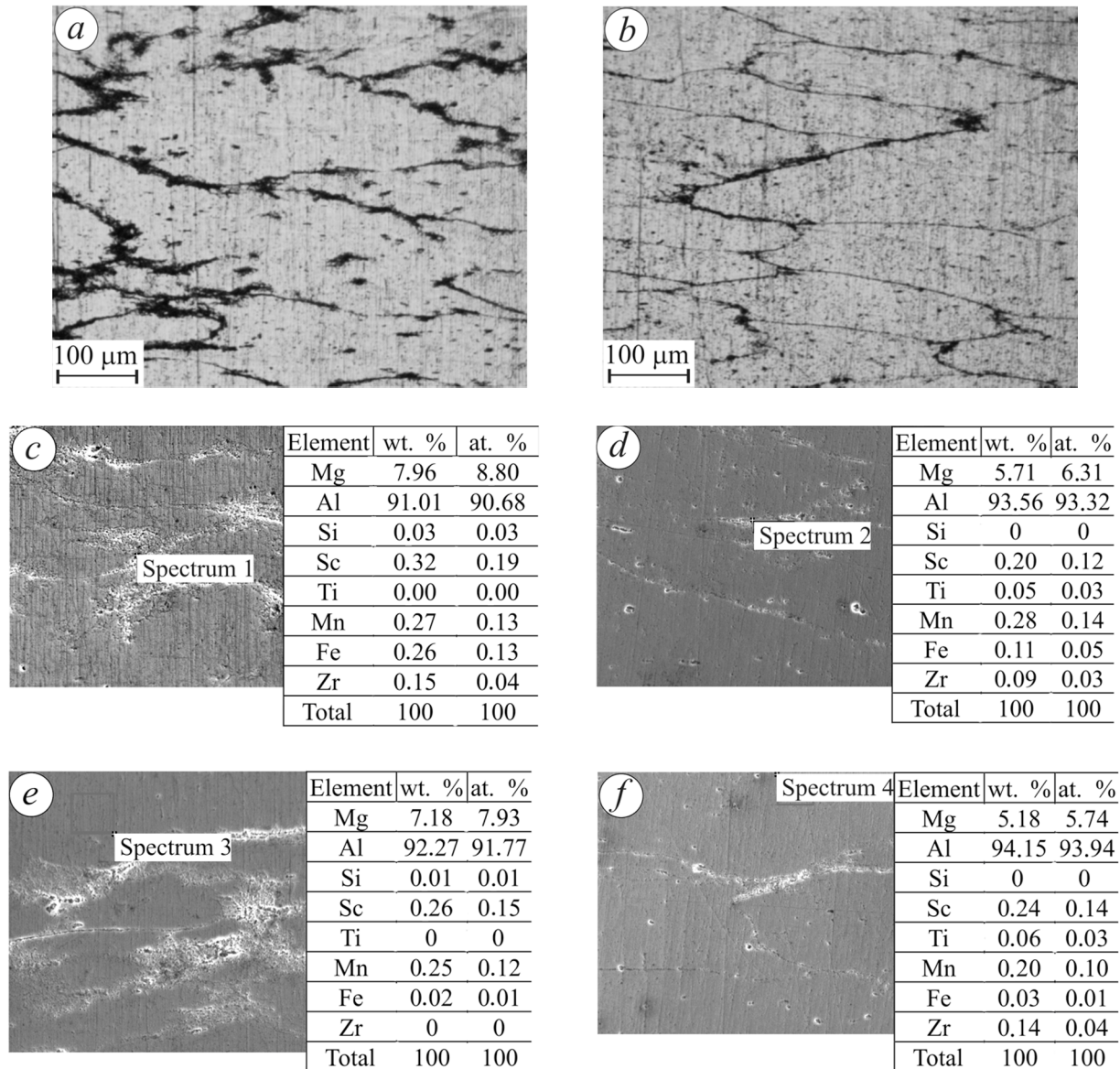


Fig. 2. Microstructures (a, b) and local chemical compositions of the precipitated intermetallic compounds (c, d) and the matrix (e, f) for alloys No. 1 (a, c, e) and No. 2 (b, d, f) after rolling.

The difference was established by analyzing their matrices. Indeed, in alloy No. 1, zirconium is absent (Fig. 2e), whereas in alloy No. 2, it is present (Fig. 2f). This means that, in the first case, the secondary Al_3Sc phase precipitates in the matrix. At the same time, in the second case, we observe the $\text{Al}_3(\text{Sc}_{1-x}\text{Zr}_x)$ phase, which is more finely divided and, hence, strengthens the alloy more efficiently [1, 2]. A similar result was earlier obtained by the authors for the alloy with lowered magnesium content in the as-cast state [5] and by other researchers for a thermally deformed alloy [12].

The elevated strength of alloys of the Al–Mg–Sc system is attained, first of all, by alloying with scandium, which leads to their structural strengthening as a result of grain refining, which is described by the Hall–Petch equation. However, it is known [14] that the grain size ambiguously affects the strength and FMGR characteristics of structural materials. In particular, the dependences for the yield strength and fatigue threshold

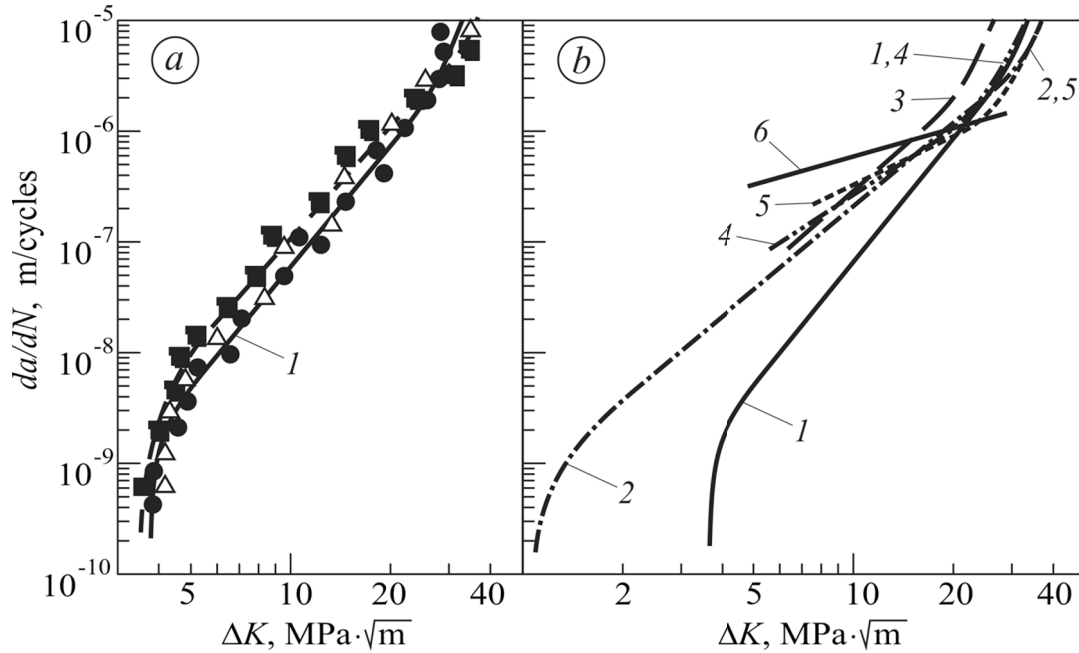


Fig. 3. Diagrams of fatigue macrocrack growth rates: (a) for rolled alloys No. 1 (●, △) and No. 2 (■) under tensile (●) and bending loading (△, ■); (b) comparison with the literature data for thermally deformed 1570-type alloys: (1) alloy No. 1, $D_{gr} = 50\text{--}150 \mu\text{m}$; (2) 6–10 μm [7]; (3) 70–170 μm [18]; (4) $\sim 1 \mu\text{m}$ [18]; (5) [19]; (6) [1].

are opposite [7, 15]:

$$\sigma_{YS} = \sigma_i + k_y D_{gr}^{-0.5}, \quad (1)$$

$$\Delta K_{th} = A + B D_{gr}^{0.5}, \quad (2)$$

where D_{gr} is the grain size and σ_i , k_y , A , and B are material constants. The characteristic ΔK_{th} is important for the evaluation of the durability of structural elements because it directly correlates with the fatigue macrocrack initiation resistance and the fatigue limit of the materials [16].

The diagrams of fatigue macrocrack growth rates indicate (Fig. 3a) that, after rolling, alloy No. 1 has a somewhat higher FMGR in the medium-amplitude part of the diagram and a lower FMGR in the high-amplitude region than alloy No. 2. Note that the diagram plotted for alloy No. 1 (by analogy with the well-known results from [17]) is independent of the geometry and loading mode of the specimen, i.e., it can be regarded as a characteristic of the material. Both alloys have high fatigue macrocrack growth resistances, which is explained by the high-energy micromechanisms of their fracture, by a fatigue striation micromechanism for $\Delta K \approx 15 \text{ MPa}\sqrt{\text{m}}$ (Figs. 4a, b) and a predominantly pitting micromechanism at $\Delta K \approx 25 \text{ MPa}\sqrt{\text{m}}$ (Figs. 4c, d).

Both alloys with relatively large grains ($D_{gr} = 50\text{--}150 \mu\text{m}$) have fairly high fatigue thresholds $\Delta K_{th} = 3.3\text{--}3.8 \text{ MPa}\sqrt{\text{m}}$, which differs them from the known alloys (Fig. 3b; curve 1 cf. curve 2). Indeed, for 1570 alloy with fine grains ($D_{gr} = 6\text{--}10 \mu\text{m}$), we have $\Delta K_{th} = 1.1 \text{ MPa}\sqrt{\text{m}}$ [7], which confirms our observations. In the high-amplitude region ($\Delta K = 15\text{--}35 \text{ MPa}\sqrt{\text{m}}$), these diagrams are in good agreement with the results of the other authors (Fig. 3b). They also indicate (curves 4 and 6) that the alloys with fine grains ($D_{gr} \sim 1 \mu\text{m}$) have low FMGR in the near-threshold region of the diagram ($\Delta K < 5 \text{ MPa}\sqrt{\text{m}}$). Therefore, in view

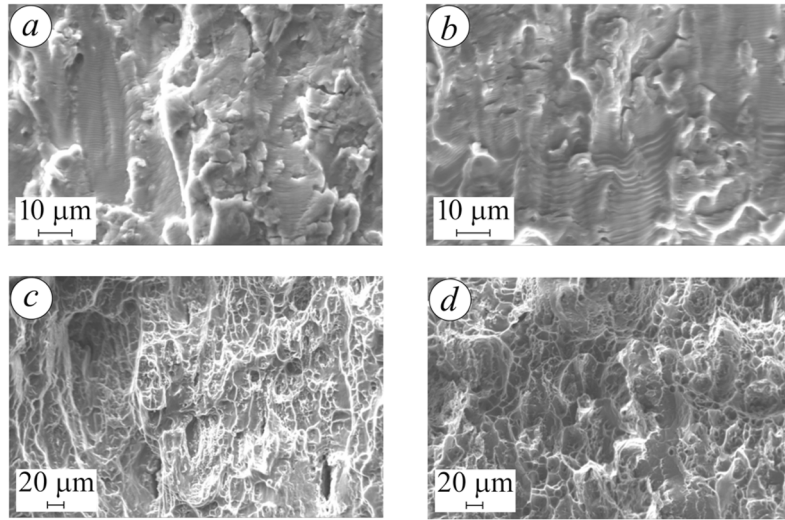


Fig. 4. Microfractograms of the specimens of alloys No. 1 (a, c) and No. 2 (b, d) for $\Delta K = 15$ (a, b) and $25 \text{ MPa}\sqrt{\text{m}}$ (c, d).

Table 3
Mechanical Characteristics and the Parameter of Structural Strength of Aluminum Alloys

No.	Alloy (alloying system)	State of the alloy	σ_{UTS} , MPa	ΔK_{th}	ΔK_{fc}	$P \cdot 10^{-3}$, $\text{MPa}^3 \cdot \text{m}$
				$\text{MPa}\sqrt{\text{m}}$		
1	No. 1 (Al–Mg–Sc)	Hot rolling	450	3.8	33	56.43
2	No. 2 (Al–Mg–Sc)	Hot rolling	396	3.4	35	47.12
3	01570 [7] (Al–Mg–Sc)	Hot rolling, annealing	410	1.1	35	15.79
4	AMg5M [20] (Al–Mg)	Hot rolling, annealing	315	3.2	33	33.26
5	D16M [20] (Al–Cu–Mg)	Hot rolling, annealing	235	3.5	32	26.32
6	D16T [20] (Al–Cu–Mg)	Hot rolling, annealing, natural aging	415	3.2	34	45.15

of the ambiguous influence of structure on the strength and FMGR of alloys of the Al–Mg–Sc system, it is necessary to analyze their mechanical behavior under the operating conditions by using the complex parameter of structural strength P (Table 3).

Among aluminum alloys of different alloying systems, alloy No. 1 is characterized by the highest value of the parameter P . For alloy No. 2, the value of P is lower but almost equal to the value obtained for the D16T high-strength alloy and higher than for the AMg5M medium-strength alloy, which is extensively used

in the aerospace industry. Note that the fine-grained structure of the alloy causes its very low fatigue threshold ΔK_{th} and, hence, determines the lowest value of the parameter P despite a relatively high strength of this alloy (position 3 in Table 3). Thus, it is clear that alloys of the Al–Mg–Sc system must have a mean grain size of several tens of micrometers in order to guarantee their elevated structural strength.

CONCLUSIONS

It was shown that, for lower magnesium content, the 1545-type alloy of the Al–Mg–Sc system thermally deformed by rolling has smaller grains and lower amounts of precipitated primary grain-boundary intermetallic compounds as compared with 1570-type alloy with a higher magnesium content. In the first case, the $Al_3(Sc_{1-x}Zr_x)$ secondary phase precipitates in the matrix. At the same time, in the second case, we observe the precipitation of the Al_3Sc phase. The temperature of thermomechanical treatment of the alloys should be $\leq 420^\circ C$. In view of the fact that the grain size exerts qualitatively opposite influence on the strength and fatigue macrocrack growth resistance of the alloys of this system, their mechanical behavior under the operating conditions should be evaluated according to the complex parameter of structural strength P .

The present work was financially supported by the target program of scientific investigations of the Department of Physical and Technical Problems of Materials Science of the NASU “Promising Structural and Functional Materials with Long-Term Service Life, Fundamentals of Their Manufacturing, Joining, and Treatment” (Project III-137-17).

REFERENCES

1. Yu. A. Filatov, V. I. Yelagin, and V. V. Zakharov, “New Al–Mg–Sc alloys,” *Mater. Sci. Eng.*, **A280**, 97–101 (2000).
2. A. Ya. Ishchenko and T. M. Labur, *Weldable Aluminum Alloys with Scandium* [in Russian], KVITs, Kyiv (1999).
3. A. V. Bronz, V. I. Efremov, A. D. Plotnikov, and A. G. Chernyavskii, “1570S alloy as a material for pressurized structures of advanced reusable vehicles of the “Energiya” rocket-space complex,” *Kosmich. Tekh. Tekhnol.*, **7**, No. 4, 62–67 (2014).
4. M. T. Fernandes, *Aluminium–Magnesium–Scandium Alloys with Hafnium*, Patent PCT/US00/19559 (Int. Publication Number WO 01/12868 A1), Publ. on 22.02.2001.
5. O. P. Ostash, S. L. Polyvoda, A. V. Narivskiy, R. V. Chepil, V. Ya. Podhurska, and V. V. Kulyk, “Influence of chemical composition on the structure, mechanical, and corrosion properties of cast alloys of the Al–Mg–Sc system,” *Fiz.-Khim. Mekh. Mater.*, **56**, No. 4, 122–127 (2020); **English translation:** *Mater. Sci.*, **56**, No. 4, 570–576 (2020).
6. L. P. Puzhailo, S. L. Polyvoda, O. V. Siryi, and O. M. Hordynya, *Melting and Casting Complex for the Semicontinuous Casting of Ingots of Aluminum Alloys* [in Ukrainian], Patent of Ukraine No. 119406, Publ. on 25.09.17, Bull. No. 18.
7. O. P. Ostash, E. M. Kostyk, V. G. Kudryashov, I. M. Andreiko, and I. A. Skotnikov, “Low-temperature cyclic cracking resistance of high-strength aluminum alloys in crack initiation and growth stages,” *Fiz.-Khim. Mekh. Mater.*, **26**, No. 3, 40–49 (1990); **English translation:** *Sov. Mater. Sci.*, **26**, No. 3, 281–288 (1990).
8. O. P. Ostash, O. A. Haivorons’kyi, V. D. Poznyakov, and V. V. Kulyk, *Method of Thermal Treatment of High-Strength Low-Alloy Carbon Steels* [in Ukrainian], Patent of Ukraine No. 105440, Publ. on 25.03.2016, Bull. No. 6.
9. O. P. Ostash, T. M. Labur, Yu. V. Holovatyyuk, V. V. Vira, V. A. Koval, V. S. Shynkarenko, and M. R. Yavorska, “Structural strength of welded joints of thermally hardened alloy of the Al–Cu–Mg system,” *Fiz.-Khim. Mekh. Mater.*, **55**, No. 4, 81–87 (2019); **English translation:** *Mater. Sci.*, **55**, No. 4, 548–554 (2020).
10. *Standard Test Method for Measurement of Fatigue Crack Growth Rates:* ASTM Standard E647 (2002).
11. A. G. Gavras, B. F. Chenelle, and D. A. Lados, “Effects of microstructure on the fatigue crack growth behavior of light metals and design considerations,” *Matéria (Rio J.)*, **15** (2), 319–329 (2010).
12. D. Zhemchuzhnikova, A. Mogucheva, and R. Kaibyshev, “Mechanical properties of Al–Mg–Sc–Zr alloys at cryogenic and ambient temperatures,” in: H. Weiland, A. Rollett, and W. Cassada (editors), in: *Proc. of the 13th Int. Conf. on Aluminum Alloys (ICAA13)*, The Minerals, Metals and Materials Series, Springer (2012), pp. 879–884.
13. A. Mogucheva, E. Babich, and R. Kaibyshev, “Microstructure and mechanical properties of an Al–Mg–Sc–Zr alloy subjected to extensive cold rolling,” in: H. Weiland, A. Rollett, and W. Cassada (editors), *Proc. of the 13th Internat. Conf. on Aluminum Alloys (ICAA13)*, The Minerals, Metals and Materials Series, Springer (2012), pp. 1773–1778.

14. O. N. Romaniv, “A structural concept of the fatigue limit of structural alloys,” *Fiz.-Khim. Mekh. Mater.*, **22**, No. 1, 106–116 (1986); **English translation:** *Sov. Mater. Sci.*, **22**, No. 1, 103–112 (1986).
15. O. P. Ostash, E. M. Kostyk, and I. N. Levina, “Effect of low temperature on the initiation and growth of fatigue cracks in 08kp steel with different grain size,” *Fiz.-Khim. Mekh. Mater.*, **24**, No. 4, 63–71 (1988); **English translation:** *Sov. Mater. Sci.*, **24**, No. 4, 385–392 (1989).
16. O. P. Ostash, “New approaches in fatigue fracture mechanics,” *Fiz.-Khim. Mekh. Mater.*, **42**, No. 1, 13–25 (2006); **English translation:** *Mater. Sci.*, **42**, No. 1, 5–19 (2006).
17. A. D. Ivasyshyn and B. D. Vasylyv, “Effect of the size and form of specimens on the diagram of growth rates of fatigue cracks,” *Fiz.-Khim. Mekh. Mater.*, **37**, No. 6, 119–120 (2001); **English translation:** *Mater. Sci.*, **37**, No. 6, 1002–1004 (2001).
18. E. Avtokratova, O. Sitdikov, R. Kaibyshev, and Y. Watanabe, “Fatigue crack growth behavior of ultrafine-grained Al–Mg–Sc alloy produced by ECAP,” *Mater. Sci. Forum*, **584–586**, 821–826 (2008).
19. M. Li., Q. Pan, Y. Wang, and Y. Shi, “Fatigue crack growth behavior of Al–Mg–Sc alloy,” *Mater. Sci. Eng.*, **A598**, 350–354 (2014).
20. Y. V. Holovatyuk, A. H. Poklyats’kyi, O. P. Ostash, and T. M. Labur, “Elevation of the structural strength of welded joints of sheets made of alloys of the Al–Cu–Mg system,” *Fiz.-Khim. Mekh. Mater.*, **54**, No. 3, 112–119 (2018); **English translation:** *Mater. Sci.*, **54**, No. 3, 412–420 (2018).